Binding of human coronary artery endothelial cells to plasma-treated titanium dioxide nanotubes of different diameters

Ajda Flašker,[1][†]* Mukta Kulkarni,[1][†] Katjuša Mrak-Poljšak,[2] Ita Junkar,[3] Saša Čučnik,[2,4] Polona Žigon,[2] Anca Mazare,[5] Patrik Schmuki,[5] Aleš Iglič,[1] Snezna Sodin-Semrl[2,6]

[1]Laboratory of Biophysics, Faculty of Electrical Engineering, University of Ljubljana, Ljubljana SI-1000, Slovenia
[2]Department of Rheumatology, University Medical Centre Ljubljana, Ljubljana SI-1000, Slovenia
[3]Josef Stefan Institute, Jamova 39, Ljubljana 1000, Slovenia
[4]Faculty of Pharmacy, Chair for Clinical Biochemistry, University of Ljubljana, Ljubljana SI-1000, Slovenia
[5]Department of Materials Science and Engineering, WW4-LKO, University of Erlangen Nuremberg, Martensstr, 7, 91058 Erlangen, Germany
[6]Faculty of Mathematics, Natural Science and Information Technologies, University of Primorska, Koper SI-6000, Slovenia

Abstract: Nanoscale topography in improving vascular response *in vitro* was established previously on various titanium surfaces. In the present study different surface nanotopographies that is different diameters of titanium dioxide (TiO$_2$) nanotubes (NTs) were fabricated by electrochemical anodization and conditioned with highly reactive gaseous oxygen plasma. The morphology of different diameter NTs was studied by scanning electron microscopy and atomic force microscopy, while changes in chemical composition on the surface before and after plasma treatment were determined by X-ray photoelectron spectroscopy. Performance of human coronary artery endothelial cells (HCAEC) on those conditioned surfaces was studied in regard to cell proliferation, released IL-6 protein and immunofluorescence microscopy (IFM). We show that HCAEC function is dependent on the diameter of the TiO$_2$ NTs, functioning far less optimally when bound to 100 nm TiO$_2$ NTs as compared to Ti foil, 15 nm NTs or 50 nm NTs. There were improved, morphological cell shape changes, observed with IFM, between HCAEC growing on oxygen-rich plasma-treated versus nontreated 100 nm NTs. These endothelialized conditioned Ti nanosurfaces could elucidate optimization conditions necessary for vascular implants in coronary arteries. © 2016 Wiley Periodicals, Inc. J Biomed Mater Res Part A: 104A: 1113–1120, 2016.

Key Words: titanium nanotubes, human coronary endothelial cells, surface plasma treatment, IL-6 protein, stents

INTRODUCTION

Coronary artery disease presents the major cause of mortality in the modern world. The majority of percutaneous coronary interventions involve stents, which are implemented in order to help enlarge the lumen wall and restore the blood flow through the affected vessel. Stents are made of hemocompatible and durable material such as titanium (Ti), 316 L stainless steel (SS-medical grade), Nitinol (an alloy of Nickel and Titanium), and Cobalt-Chromium (CoCr). In some instances, a stent can elicit allergic reactions most commonly those that contain Nickel, such as Nitinol and stainless steel.[1,2] The most promising properties of titanium and titanium alloys, more specifically high biocompatibility, resistance to body fluids, great tensile strength, flexibility, and high corrosion resistance, have ensured their successful and extensive use as biomaterials,[3,4] for example materials in stents. For >50 years, metallic materials have been used in medical applications (orthopaedics, vascular surgery, and dentistry) and titanium (Ti) and Ti alloys received significant attention in stents applications.[3–6] The stents can be divided in bare metal stents (BMS) and drug-eluting stents (DES). With DES the problems of allergenic reactions as well as risks of restenosis were lowered, as DES release anticell-proliferative, immunosuppressive or antithrombogenic drugs which inhibit proliferation of smooth muscle cells and reduce thrombus formation.[7] Titanium in its oxide

TABLE I. Anodization Conditions used for Fabrication of Ti-Nanostructures.

Diameter of Nanotubes	Electrolyte Solution	Potential	Time
15 nm	EG + 8M H_2O + 0.2M HF	10 V	2.5 h
50 nm	EG + 8M H_2O + 0.2M HF	20 V	2.5 h
100 nm	EG + 8M H_2O + 0.2M HF	58 V	2.5 h

EG: ethylene glycol; HF: hydrogen fluoride.

form has been proposed, because of its excellent tissue response, as a suitable stent coating on bare metal stents, providing a hemocompatible surface, with alterations in its surface chemistry and topography contributing to improved biocompatibility.[8–15] Success of stents depends mainly on avoiding the aggregation of platelets, preventing uncontrolled proliferation of smooth muscle cells and appropriate proliferation of endothelial cells. As the endothelial cells are thought to be an ideal natural antithrombogenic material, which is found in our natural blood vessels it would be valuable to produce such stent surfaces which would improve proliferation of endothelial cells. Research in the field of nanomaterials has revealed that the material's topography is a crucial factor for appropriate biological response. Nanoscale surface topography stimulates and controls several molecular and cellular events at the tissue/implant interface has prompted investigations of such topographies in the design of implantable metals.[16–18] Nanomodification of Ti generating patterened TiO_2 surfaces has proved beneficial in promoting endothelial proliferation as well as migration onto stent surfaces.[8–11] Stent surfaces that promote re-endothelialization would be a good option for preventing stent thrombosis after long-term implantation. The previous study[8] on flat Ti surfaces successfully demonstrated that uniform TiO_2 nanoscale modifications of various topologies on metallic Ti promoted endothelialization, with subsequent inhibition of smooth muscle cell proliferation and platelet adhesion. For nanopatterening of the Ti surfaces, it has been proved that electrochemical anodization is the best suitable method to obtain desired morphologies.[4,19,20]

Recently, our group investigated the binding of specific plasma proteins (e.g. immunoglobulin G, acute phase serum amyloid A (SAA) and β2-glycoprotein I) under different conditions onto titanium dioxide foil and nanotubes (NTs) of different diameters. We found that protein attachment can be correlated with larger NT diameters and presumably lengths of NTs, which could impact the growth of cells, physiological blood-nanomaterial interface, and hemocompatibility responses.[6] Previously, we had determined that human primary endothelial cells coming from different sources, such as coronary arteries (HCAEC) or umbilical veins (HUVEC) have very unique responses to inflammatory stimuli, with HCAEC being highly responsive and eliciting significantly increased interleukin-6 (IL-6) at both the mRNA and protein levels.[21,22] HCAEC also exhibited highly elevated expression of TLR2 following stimulation by either IL-1β or SAA and showed upregulated phosphorylation of ERK1/2, NF-κB (p65, p105) and JNK, as well as expression/

release of IL-6, IL-8, G-CSF, GM-CSF, ICAM-1 and VCAM-1, all potent molecules involved in neutrophil-related activities in response to SAA.[23]

In the present work, Ti surfaces were nanostructured by electrochemical anodization into different diameters TiO_2 NTs. The experimental anodization conditions (electrolyte composition, applied voltage, time) were chosen to obtain a specific surface topography, that is a specific diameter (15, 50, or 100 nm), with an open top morphology. The obtained nanostructures were surface conditioned with highly reactive oxygen plasma in order to remove impurities from the surface and to increase oxygen content on the surface. The influence of nanotexturing of Ti substrates with surface conditioning was studied in order to determine the performance of HCAEC on NTs and their functionality, which can elucidate their potential use for vascular implants in coronary arteries. Our overall aim was to determine whether plasma-treated or untreated TiO_2 NTs (of different diameters) could provide an appropriate support for HCAEC optimal growth, proliferation, and overall cellular well-being.

MATERIALS AND METHODS
Growth of TiO_2 NTs by electrochemical anodization
TiO_2 nanostructures were obtained by electrochemical anodization of titanium foils (Advent Research Materials, England, 0.1 mm thickness, 99.6% purity) following a previously published procedure.[6] Briefly, prior to anodization, the Ti foils were cleaned by successive ultrasonication in acetone, ethanol, and deionized (DI) water for 5 min each and then dried in a nitrogen stream. Ethylene glycol (EG) based electrolytes were used to grow Ti-nanostructures with specific compositions of water (H_2O) and hydrofluoric acid (HF) and optimized experimental parameters (such as applied voltage and time)—as listed in Table I. All anodization experiments were carried out at room temperature (~20°C) in a two-electrode system with titanium foil as the anode and platinum gauze as the cathode, with a working distance of 15 mm.

Formed nanostructures were kept in ethanol for 2 hours to remove all organic components from the electrolyte, then washed with distilled water and dried in a nitrogen stream.

Scanning electron microscopy
The morphology of the obtained TiO_2 nanostructures was observed using a field-emission scanning electron microscope—Hitachi FE-SEM S4800 as previously described.[24] High contrast images of nanostructural morphology of Ti-surfaces were obtained without gold sputtering, as the untreated samples already display images with reasonably good contrast.

Gaseous plasma treatment of NTs
Treatment of NTs was done by oxygen plasma in the plasma reactor shown in Figure 1. The system was evacuated with a two-stage oil rotary pump with a nominal pumping speed of 4.4×10^{-3} m^3/s. The discharge chamber was a Pyrex cylinder with a length of 0.6 m and an inner diameter of 0.036 m. Gaseous plasma was created with an inductively
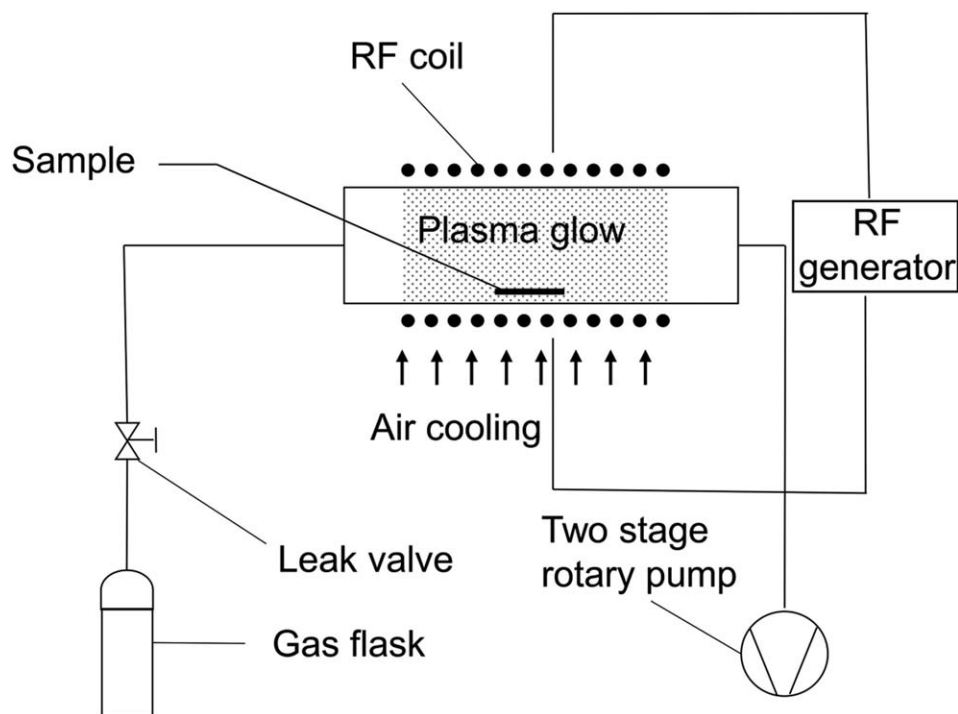
FIGURE 1. The experimental setup for treatment of samples with radiofrequency (RF) plasma. The setup consists of the gas flask with oxygen, leak valve, plasma chamber with RF coil and the air cooling system, RF generator and a two-stage rotary pump.

coupled radiofrequency (RF) generator, operating at a frequency of 13.56 MHz and an output power of about 200 W. The plasma parameters were measured with a double Langmuir probe and a catalytic probe. Commercially available oxygen was leaked into the discharge chamber. The pressure was measured by an absolute vacuum gauge. The pressure was adjusted during continuous pumping by a precise leak valve. In our experiments, the pressure was fixed at 75 Pa, because at this pressure we obtained the highest degree of dissociation of oxygen molecules as measured by the catalytic probes.[25] At these discharge parameters, plasma with an ion density of about 2×10^{15} m^{-3}, an electron temperature of 4 eV, and a neutral atoms density of about 4×10^{21} m^{-3} was obtained. The samples were treated for 60 s.

Atomic force microscopy

Topography of Ti-foil and as formed Ti-nanostructured surfaces were examined by Atomic Force Microscopy (Solver PRO, NT-MDT, Russia) in tapping mode in air. The samples were scanned with the standard Si cantilever at a constant force of 22 N/m and resonance frequency of 325 kHz (10 nm tip radius, 95 μm tip length). The average surface roughness (Ra) was calculated from 1×1 μm^2 image areas.

X-ray photoelectron spectroscopy

The surface of the sample was analyzed with an X-ray photoelectron spectroscopy (XPS) instrument TFA XPS Physical Electronics. The base pressure in the XPS analysis chamber was about 6×10^{-8} Pa. The samples were excited with X-rays over a 400-μm spot area with a monochromatic Al

$K_{\alpha1,2}$ radiation at 1486.6 eV. The photoelectrons were detected with a hemispherical analyzer positioned at an angle of 45° with respect to the normal of the sample surface. The energy resolution was about 0.5 eV. The XPS spectra were measured on plain titanium, on NTs (with 15, 50, and 100 nm in diameter) immediately after anodization procedure and on NTs (with 15, 50, and 100 nm in diameter) immediately after plasma treatment.

Cell culturing

Human coronary artery endothelial cells (HCAEC) were purchased from Lonza(Walkersville, MD, USA). HCAEC were grown under standard conditions in Endothelial Growth Medium-2 (EGM-2; Lonza, Walkersville, MD, USA) supplemented with singlequots EGM-2-MV with 5% fetal bovine serum, at 37°C in 5% CO_2 in humidified air. HCAEC were passaged using Trypsin/EDTA and used for experiments at low passages 4 and 5. A summary of the work flow is provided (Scheme 1).

Immunofluorescent microscopy and cell morphology

For immunochemistry determination, HCAEC were applied onto NTs with different diameter pore sizes (100, 50, and 15 nm) and foil, all in the presence or absence of plasma, in 12 well plates at a density of 15×10^3 cells per cm^2. Cells were grown for 3 days, then stained with the fluorescent dyes Fluorescein Phalloidin and DAPI (both from Molecular Probes, Thermo Fisher Scientific) with affinity for F-actin and the nucleus, respectively, following manufacturer's instructions. Briefly, for fluorescein phalloidin staining cells were washed twice for 3 min with prewarmed phosphate-
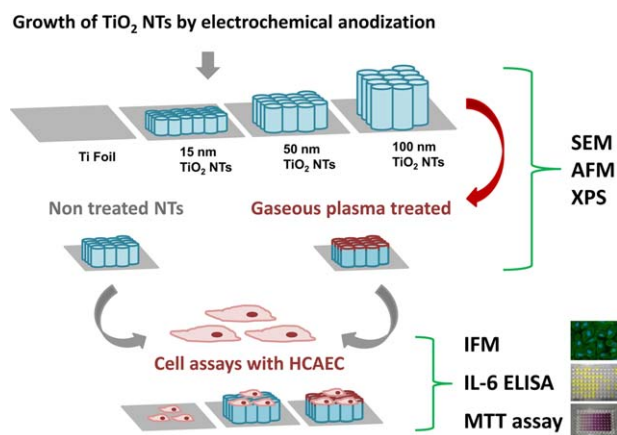
SCHEME 1. Summary of work flow
The sequential working protocols involved were initially: production of titanium dioxide (TiO_2) nanotubes (NTs) with different diameters by electrochemical anodization and characterization of their surface morphology by scanning electron microscopy (SEM) and atomic force microscopy (AFM). This was followed by the investigation of the chemical composition and changes between plasma-treated and untreated foil and NTs of different diameters by X-ray photoelectron spectroscopy (XPS). Cellular protocols were performed lastly, in order to determine cell viability, proliferation and well-being, with the following experiments: immunofluorescent microscopy (IFM), interleukin-6 (IL-6) enzyme-linked immunosorbant assay (ELISA) and the cell proliferation MTT (3-(4,5-dimethylthiazol-2-yl)-2,5-diphenyltetrazolium bromide) assay.

buffered saline (PBS, pH 7.4) and fixed in 3.7% formaldehyde solution in PBS for 10' at RT, followed by washing three times for 3 min with PBS at RT. Cells were then treated with a solution of 0.1% Triton X-100 in PBS for 4 min and washed with PBS for three times, 3 min. Fluorescein Phalloidin (methanolic stock solution) was diluted 1:40 in PBS containing 1% BSA and cells on NTs incubated for 30 min. The wells were covered to prevent evaporation. Additional washing was performed three times, 3 min with PBS.

For DAPI staining, DAPI stock solution was diluted to a final concentration of 300 nM in PBS and was added to the NT preparations, making certain that the cells were completely covered and incubated for 5 min, followed by a 3 min wash with PBS. All treatments and washes were performed at RT. A drop of SlowFade reagent (Thermo Fisher Scientific, USA) was then applied onto the cells/NT preparation and adjusted with a cover slide using clear nail polish. The slides can be examined immediately or stored in the dark at 2–6°C for next day examination. Cell staining and morphology was evaluated using the fluorescent microscope Nikon eclipse E400 and *images were* taken with a digital camera (*Nikon* Instruments, Dusseldorf, Germany) and *Nikon ACT-1* imaging software.

Cell proliferation assay

HCAEC were seeded into 12 well plates at a density of 15 $\times$ 10^3 cells per cm^2 in presence and absence of treated/nontreated NTs. After 3 days, the CellTiter 96 Aqueous One Solution Cell Proliferation Assay (MTT; Promega, Madison, WI, USA) was used to determine cell proliferation, following

manufacturer's instructions. Briefly, 20 μL of reagent MTS (3–(4,5-dimethylthiazol-2-yl)-5–(3-carboxymethoxyphenyl)-2–(4-sulfophenyl)-2H-tetrazolium) was added into every 100 μL of cell medium EGM-2. Enough reagent/medium was added into wells to cover the cells in duplicate and incubated at 37°C, 5% CO_2 for 20 min. One hundred μL of supernatant was pipetted into 96 well plates and the yellow tetrazolium MTT compound (3–(4, 5-dimethylthiazolyl-2)-2, 5-diphenyltetrazolium bromide) was reduced by metabolically active cells to generate reducing equivalents. The resulting intracellular purple formazan was quantified by absorbance recorded at 490 nm. In order to normalize the results against the background control (which included only
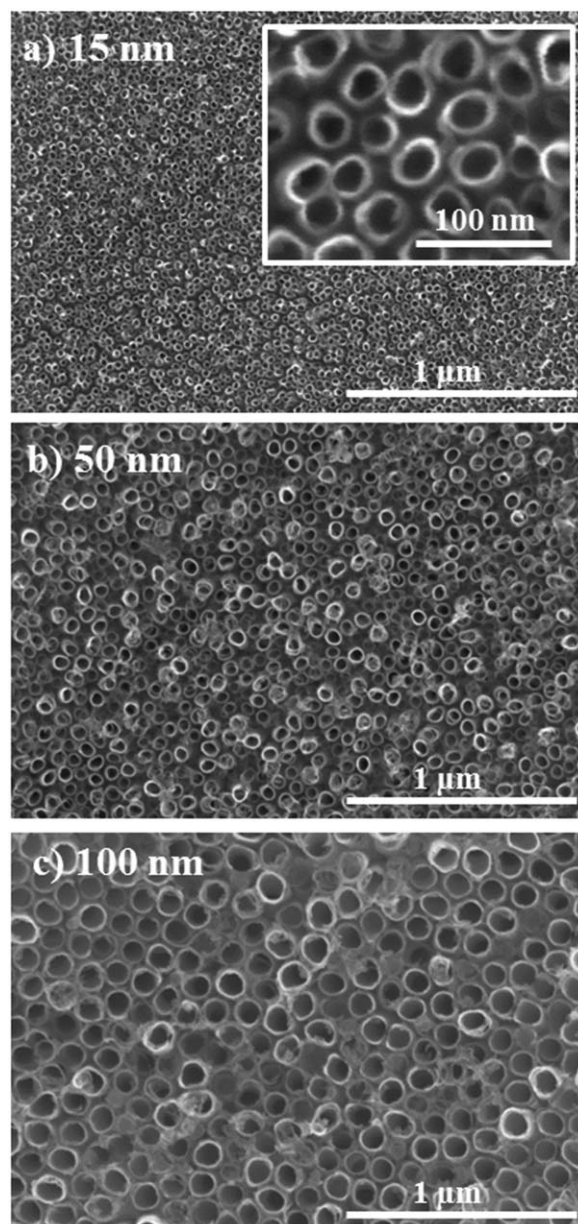

FIGURE 2. Top view SEM images of TiO_2 NTs with (a) 15 nm diameter (inset shows a higher magnification top view image), (b) 50 nm diameter, and (c) 100 nm diameter.
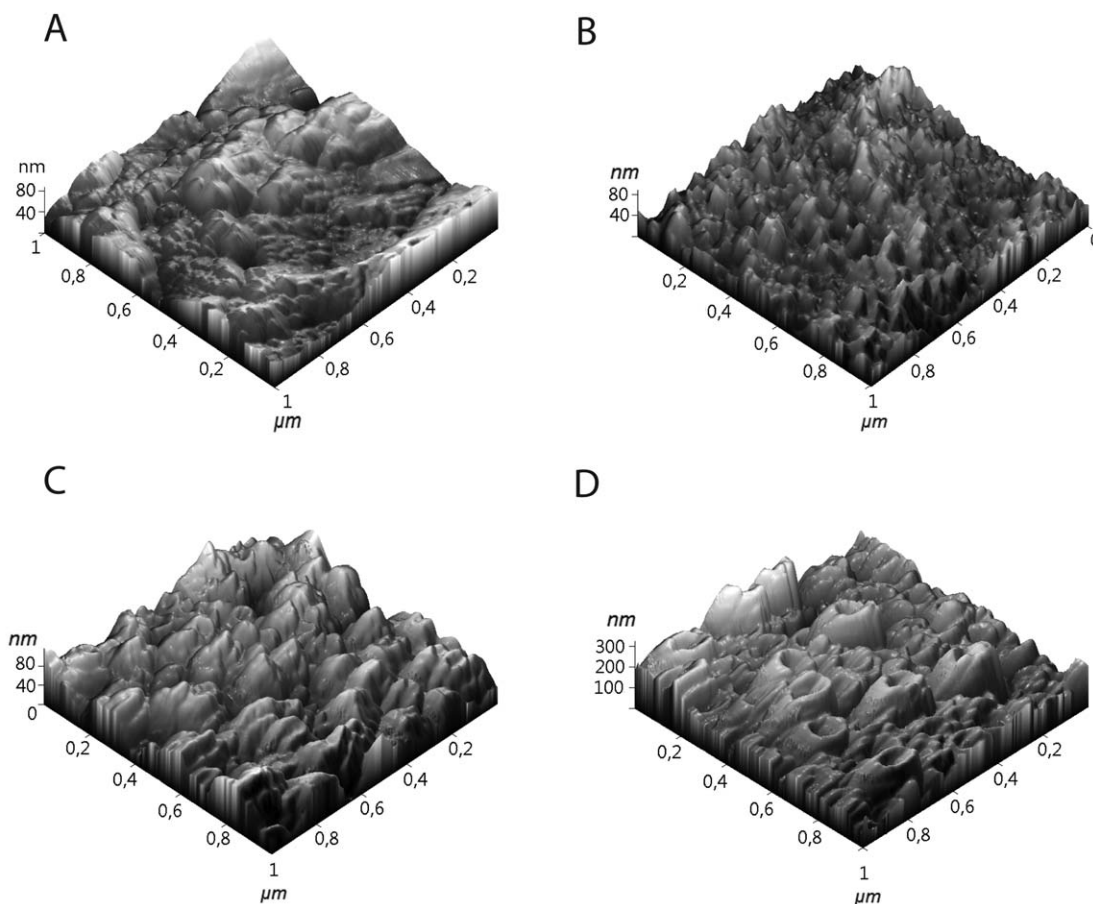
FIGURE 3. Surface morphology by AFM on (a) Ti-foil, (b) 15 nm NTs, (c) 50 nm NTs, and (d) 100 nm NTs.

medium and assay reagent) we deducted the background absorbance values from the results.

Measurement of human interleukin-6 released protein levels

HCAEC supernatants were collected 24 h after starting cell treatments and centrifuged for 3 min at 5000 rpm, aliquoted and stored at −20°C. Samples were thawed, allowed to reach room temperature and diluted 1:50 in standard dilution buffer. Released IL-6 protein levels were determined in duplicate by enzyme-linked immunosorbent assay (ELISA) (Invitrogen, Belgium), following manufacturer's instructions. Statistical analysis was performed using analysis of variance, using the mean+/-SD of three separate experiments.

RESULTS

Nanoscale morphology of TiO_2 NTs

The nanoscale morphology of the obtained TiO_2 structures was evaluated by scanning electron microscopy (SEM), and the top view SEM images (see Fig. 2) clearly indicate that self-organized nanotubular structures with different diameters are obtained with a high degree of uniformity by electrochemical anodization. Atomic force microscopy (AFM) is used to investigate the topographical features of the NTs with different diameters and pristine (nonanodized) Ti-foil,

are shown in Figure 3. The estimated average surface roughness measured on 1×1 μm² of the Ti-foil is around 11.8 nm [Fig. 3(a)]. However, imaging of 15 nm diameter NTs is not completely representative, because of the size of the AFM tip that does not allow it to enter the 15 nm diameter NTs. This is the reason why the 15 nm diameter nanotubular feature appears to be closed instead of opened (hollow), as seen in Figure 3(b). The average surface roughness measured on 15 nm NTs is around 9.6 nm, which is a bit lower in comparison to the Ti-foil. In case of the 50 nm NTs, a similar effect is observed, as many of the tubes seem to be closed—see Figure 3(c), and a roughness of around 15.5 nm was measured. It was, however, possible to get a better understanding of the nanotubular topographic features for the 100 nm diameter structures, as shown in Figure 3(d).

XPS analysis

The chemical composition of the titanium dioxide nanotubular structures was analyzed before and after plasma treatment with XPS. Figure 4 presents an overview of the chemical composition of the different surfaces used (Ti foil, nanotubular structures and the nanotubular structures after plasma treatment). The plain titanium surface has 38.3 at % of carbon, about 41.2 at % of oxygen, and about 18 at % of
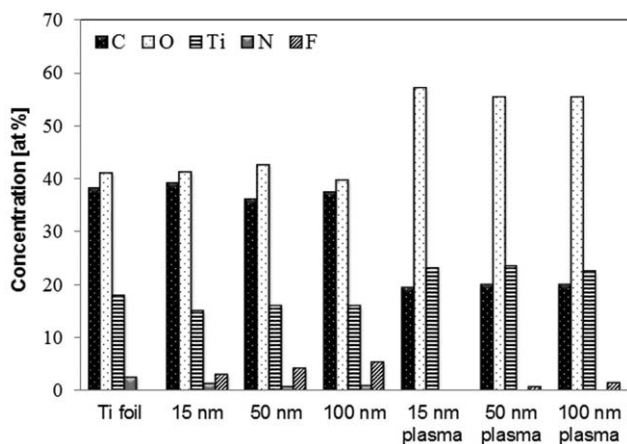
FIGURE 4. Chemical composition (at %) obtained from XPS spectra on Ti foil and on as anodized and plasma-treated TiO_2 NTs (15, 50, and 100 nm in diameter).

titanium. After the growth of NTs on this surface by anodization, we observe a slight decrease in the carbon content and increase in the fluorine content, which is because of the electrolyte used during the anodization procedure (organic electrolyte containing fluorine ions). By increasing the size of NT more fluorine is observed on the surface. Thus the F/Ti ratio increases from 0.21 to 0.33 for 15 and 100 nm diameter NTs, respectively. However after exposure to oxygen plasma only a small amount of fluorine can be detected on 50 and 100 nm NTs, while no fluorine is observed on 15 nm. For example on plasma-treated 100 nm diameter NTs the F/Ti ratio is about 0.07. All plasma-treated surfaces have lower carbon content, which decreases from about 38 at % to about 20 at %, and of course an increase in oxygen and titanium is observed.

Cell staining and morphology

In order to determine the phenotype, morphology, and general condition of the cells, HCAEC were stained with fluorescein phalloidin for F-actin and DAPI for double-stranded DNA (Fig. 5). HCAEC grown on glass appeared phenotypically healthy and in a confluent state. Cells grown on untreated or plasma-treated foil were comparable to the control. While the cells on 15 nm NTs were numerous, they appeared smaller in size and slightly rounder and were comparable with HCAEC grown on 50 nm diameter NTs. On plasma-treated 50 nm diameter NTs, the cells observed were in better condition than on the 50 nm NTs alone. However, HCAEC grown on 100 nm NTs exhibited a dramatic reduction in number, as well as a change in cell shape, many appearing to exhibit membrane blebbing indicative of apoptotic cells.

Cell proliferation

To investigate cell proliferation, the MTT assay was performed. The MTS tetrazolium compound in the MTT assay is bio-reduced by the cells into a colored formazan and measured by the absorbance at 490 nm (Fig. 6). This conversion

is accomplished by NADPH or NADH produced by dehydrogenase enzymes in metabolically active cells. Surprisingly comparable absorbance values at 490 nm were obtained between the controls (cells grown on glass and plastic surfaces) and plasma-treated and untreated NTs with 50 and 15 nm diameters and foil. One hundred nm NTs
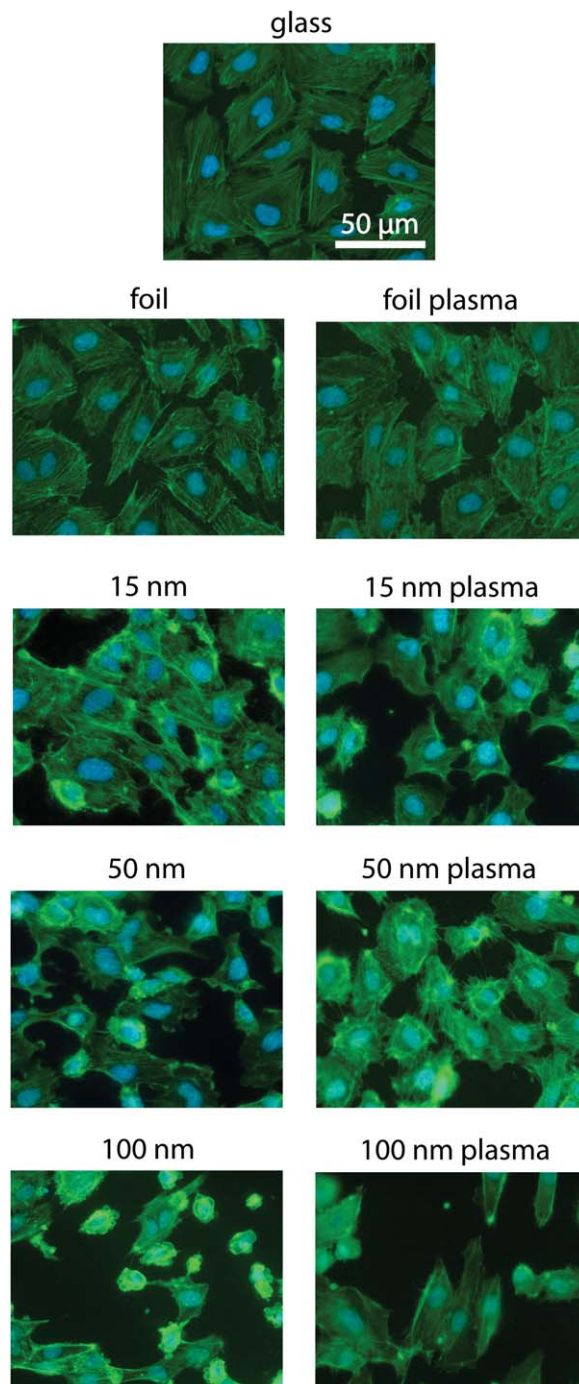

FIGURE 5. Fluorescent images of HCAEC on different surfaces. Cells were grown for 3 days on glass and untreated or plasma-treated TiO_2 NTs of different diameters (15, 50, and 100 nm). Each experiment was repeated three times and representative images are shown. F-actin is shown in green (Fluorescein Phalloidin) and nuclei are shown in blue (DAPI).
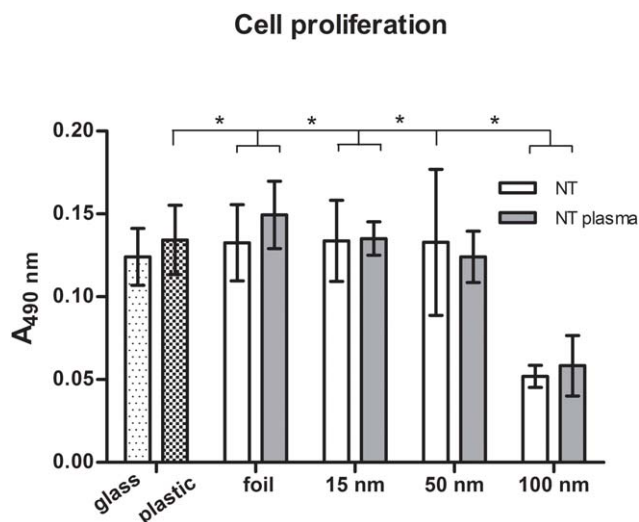
Cell proliferation

FIGURE 6. Cell proliferation was monitored by the MTT assay. Three independent experiments were performed. The results were analyzed with two-way analysis of variance and Bonferroni post-tests, and significance was determined as $*p < 0.05$. MTT, 3–(4,5-dimethylthiazol-2-yl)−2,5-diphenyltetrazolium bromide.

(plasma-treated and untreated) showed a significantly decreased cell proliferation, which is in line with our cell staining and morphology data (Fig. 5, bottom panels).

Interleukin 6 (IL-6) levels

In order to determine whether and to what extent IL-6 is released from HCAEC following the binding of cells to NTs of different diameter and/or treatments, ELISA was performed (Fig. 7). HCAEC showed strikingly increased IL-6 levels in supernatants when cells are grown on 100 nm NTs, in presence or absence of plasma treatment, while HCAEC did not exhibit change in IL-6 levels whether grown on glass or plastic surfaces.

DISCUSSION AND CONCLUSIONS

Stents used in coronary artery diseases should be stable, durable, flexible, hemo- and cell-compatible, with corrosion resistance and without the possibility of eliciting allergic reactions. With the aim to evaluate more optimal biocompatible material, we grew TiO_2 NTs of different diameters, visualized their surface morphology and determined differences between plasma-treated and untreated TiO_2 NTs based on their chemical composition and endothelial cell effects. Firstly, we evaluated TiO_2 NT surface morphology, with SEM (Fig. 2) providing an overall scan of the surface, while AFM (Fig. 3) provided a clear picture of the open top of the nanotubular structures, since the AFM tip could penetrate the inner diameter of the 100 nm diameter NTs. The evaluated surface roughness was the highest for this structure, around 41.1 nm, mainly because of the ability of the AFM tip to enter inside of the NTs. It should be noted that also in this case, the measured roughness is underestimated, as the AFM tip could not distinguish the interstitial sites among the NTs and was not able to reach the bottom of the

NT surface. Nevertheless, all the morphological features measured are beneficial to validate the presence of NTs and their variable depth in contrast to two-dimensional SEM micrographs. Therefore, the AFM study revealed slightly different information than SEM, because of its technical limitations as described above. It should also be noted that AFM analysis was done also on NTs following plasma treatment and no significant differences in surface morphology were observed (data not shown).

No significant differences in chemical composition between the plasma-treated surfaces were observed either, nor between the untreated surfaces (with the exception of fluorine content). It was shown that plasma treatment removes fluorine, as well as carbon impurities from the surface, which could be mainly because of interaction of highly reactive oxygen plasma species with the surface, by which carbon and fluorine are removed from the surface.

Since IL-6 is secreted by endothelial cells, T cells, and macrophages to stimulate an immune response, for example during infection and after trauma, especially burns or other tissue damage leading to inflammation,[26,27] this cytokine could be used as a marker of cellular stress/well-being. Because release of IL-6 is strongly correlated with the number of living cells, the results were normalized using the MTT test. Moreover, levels of IL-6 corresponded with the cell proliferation test and cell morphology data, indicating comparable results on glass, plastic, foil, and NT of 15 and 50 nm diameter (regardless of the plasma treatment). These results are in accordance with HCAEC cellular physiology, where cells make relatively close cell–cell contacts, which are prevented by the larger NT spaces in 100 nm NTs. Indeed, HCAEC grown on 100 nm NTs exhibited a dramatic reduction in number, as well as a change in cell shape, many appearing to exhibit membrane blebbing, indicative of apoptotic cells, which is in accordance with the cell proliferation results.
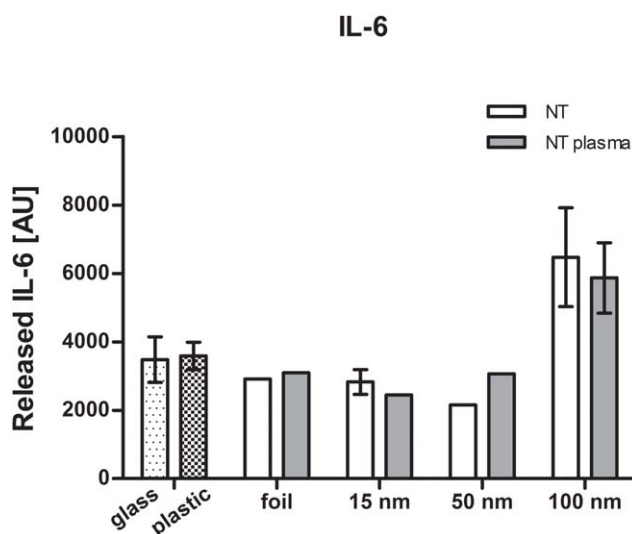
IL-6

FIGURE 7. Released IL-6 protein levels were measured in supernatants of HCAEC grown on indicated substrates for 3 days. IL-6 was determined by ELISA and expressed as arbitrary units following the normalization against cell proliferation MTT assay.

The chemical composition changes (including oxygen content) between untreated and plasma-treated TiO_2 NTs (15, 50, and 100 nm in diameter) did not significantly affect endothelial cell proliferation (Fig. 6) or released IL-6 protein levels (Fig. 7), which only strengthens the point that size of NT diameter seems to be the determining factor responsible for the cellular changes observed. However, there was an indication that plasma treatment (along with elevated oxygen content) could in fact protect cells from morphological change (e.g. membrane blebbing) (Fig. 5, bottom panels).

In conclusion, our data clearly show that there are higher rates of HCAEC membrane blebbing, increased release of IL-6 into the supernatants and significantly diminished cell proliferation observed on 100 nm NTs, all indicating the importance of diameter size and, up to a point, also surface treatment for the well-being of these specialized cells. There were less blebbing cells observed on the plasma-treated 100 nm NTs, however, this did not reflect in the quantitative assays. These results could elucidate optimization of conditions necessary for vascular implants in coronary arteries. In the future, it would be relevant to examine cellular apoptosis in greater detail, especially in regard to the plasma-treated/untreated changes. Also, it would be of interest to investigate the NTs in combination with plasma proteins and HCAEC, in order to achieve closer representation to *in vivo* conditions.

REFERENCES

1. Hanawa T. Metal ion release from metal implants. J Artif Org 2009; 12:73–79.
2. Basko-Plluska JL, Thyssen JP, Schalock PC. Cutaneous and systemic hypersensitivity reactions to metallic implants. Dermatitis 2011; 22:65–79.
3. Kulkarni M, Mazare A, Schmuki P, Iglič A. Biomaterial surface modification of titanium and titanium alloys for medical applications. Nanomedicine 2014;111–136.
4. Roy P, Berger S, Schmuki P. TiO₂ nanotubes: Synthesis and applications. Angew Chem 2011; Ed50:2904–2939.
5. Kulkarni M, Mazare A, Gongadze E, Perutkova S, Kralj-Iglic V, Milosev I, Schmuki P, Iglic A, Mozetic M. Titanium nanostructures for biomedical applications. Nanotechnology 2015; 26:062002
6. Kulkarni M, Flasker A, Lokar M, Mrak-Poljsak K, Mazare A, Artenjak A, Cucnik S, Kralj S, Velikonja A, Schmuki P, Kralj-Iglic V, Sodin-Semrl S, Iglic A. Binding of plasma proteins to titanium dioxide nanotubes with different diameters. Int J Nanomed 2015; 10:1359–1373.
7. Jack P, Chen MD, Hou D, Pendyala L, Goudevenos JA, Kounis NG. Drug-eluting stent thrombosis: The Kounis hypersensitivity-associated acute coronary syndrome revisited. JACC Cardiovasc Interv 2009; 2:583–593.
8. Mohan CC, Sreerekha PR, Divyarani VV, Nair SV, Chennazhi KP, Menon D. Influence of titania nanotopography on human vascular cell functionality and its proliferation in vitro. J Mater Chem 2012; 22:1326–1340.
9. Fine E, Zhang L, Fenniri H, Webster TJ. Enhanced endothelial cell functions on rosette nanotube-coated titanium vascular stents. Int J Nanomed 2009; 4:91–97.
10. Peng L, Eltgroth ML, LaTempa TJ, Grimes CA, Desai TA. The effect of TiO₂ nanotubes on endothelial function and smooth muscle proliferation. Biomaterials 2009; 30:1268–1272.
11. Brammer KS, Oh S, Gallagher JO, Jin S. Enhanced cellular mobility guided by TiO₂ nanotube surfaces. Nano Lett 2008; 8:786–793.
12. Tsyganov I, Maitz MF, Wieser E. Blood compatibility of titanium-based coatings prepared by metal plasma immersion ion implantation and deposition. Appl Surf Sci 2004; 235:156–163.
13. Huang N, Yang P, Cheng X, Leng Y, Zheng X, Cai G, Zhen Z, Zhang F, Chen Y, Liu X, Xi T. Blood compatibility of amorphous titanium oxide films synthesized by ion beam enhanced deposition. Biomaterials 1998; 19:771–776.
14. Windecker S, Mayer I, De Pasquale G, Maier W, Dirsch O, De Groot P, Wu Y, Noll G, Leskosek B, Meier B, Hess OM. Stent coating with titanium-nitride-oxide for reduction of neointimal hyperplasia. Circulation 2001; 104:928–933.
15. Zhang F, Zheng Z, Chen Y, Liu X, Chen A, Jiang Z. *In vivo* investigation of blood compatibility of titanium oxide films. J Biomed Mater Res 1998; 42:128–133.
16. Palmaz JC. Intravascular stents in the last and the next 10 years. J Endovasc Ther 2004; 11:II-200–II-206.
17. deMel A, Cousins BG, Seifalian AM. Surface modification of biomaterials: A quest for blood compatibility. Int J Biomater 2012; 2012:8
18. Werner C, Maitz MF, Sperling C. Current strategies towards hemocompatible coatings. J Mater Chem 2007; 17:3376–3384.
19. Kowalski D, Kim D, Schmuki P. TiO₂ nanotubes, nanochannels and mesosponge: Self-organized formation and applications. Nano Today 2013; 8:235–264.
20. Lee K, Mazare A, Schmuki P. One-dimensional titanium dioxide nanomaterials: Nanotubes. Chem Rev 2014; 114:9385–9454.
21. Lakota K, Mrak-Poljsak K, Rozman B, Kveder T, Tomsic M, Sodin-Semrl S. Serum amyloid A activation of inflammatory and adhesion molecules in human coronary artery and umbilical vein endothelial cells. Eur J Inflamm 2007; 5:73–81.
22. Lakota K, Mrak-Poljsak K, Rozman B, Sodin-Semrl S, et al. Increased responsiveness of human coronary artery endothelial cells in inflammation and coagulation. Mediators Inflamm 2009; 2009:146872
23. Lakota K, Mrak-Poljsak K, Bozic B, Tomsic M, Sodin-Semrl S. Serum amyloid A activation of human coronary artery endothelial cells exhibits a neutrophil promoting molecular profile. Microvasc Res 2013; 90:55–63.
24. Paulose M, Prakasam HE, Varghese OK, Peng L, Popat KC, Mor GK, Desai TA, Grimes CA. TiO₂ nanotube arrays of 1000 length by anodization of titanium foil: Phenol red diffusion. J Phys Chem C 2007; 111:14992–14997.
25. Cvelbar U, Mozetič M, Babič D, Poberaj I, Ricard A. Influence of effective pumping speed on oxygen atom density in a plasma post-glow reactor. Vacuum 2006; 80:904–907.
26. Kishimoto T. IL-6: from its discovery to clinical applications. Int Immunol 2010; 22:347–352.
27. Hunter CA, Jones SA. IL-6 as a keystone cytokine in health and disease. Nat Immunol 2015; 16:448–457.